

CHAPTER 40

NON-UNIFORM ALONGSHORE CURRENTS

Michael R. Gourlay *

Abstract

Alongshore gradients of breaker height have been shown to significantly influence the velocities and circulation patterns of nearshore current systems. Experimental data from an idealized laboratory experiment shows that the form of the nonuniform wave generated current system resulting from diffraction behind an offshore breakwater is essentially determined by the beach-breakwater geometry while its magnitude depends upon the wave height. Furthermore the current may produce significant increases in the magnitude of the wave set-up within the three dimensional system. For the case investigated, where the alongshore gradient of breaker height is comparatively large, the maximum mean alongshore current velocity is not greatly affected by bottom resistance and may be computed for plunging breakers from a relation of the following form;

$$\frac{V}{\sqrt{gH_b^*}} = f\left(\frac{H_b}{d_b}, \frac{x_p}{H_b}, \tan \alpha\right)$$

derived from a simple momentum analysis including "radiation stress" terms. The influence of bottom resistance can be included if necessary.

1. Introduction

The phenomenon of the uniform alongshore current caused by waves breaking at an angle to a straight beach has received a considerable amount of study (1,2). The simple case with waves of uniform height seldom occurs in nature and in practice there is often an alongshore gradient of breaker height which influences the velocity and form of the alongshore current (3). Indeed it is now generally accepted that rip currents are produced by regular alongshore variations in the breaker height (4,5). Moreover it is possible, when the approaching wave crests are parallel to the coast, that the current velocity and circulation pattern are almost completely determined by alongshore breaker height gradients (6).

In the vicinity of coastal structures and coastal features such as reefs and headlands it has been found that wave generated current systems are very much influenced by variations both in the breaker height in the alongshore direction and in the location of the break point relative to those structures and/or features which determine the local coastal geometry (7). In general, any nearshore wave generated current system where breaker height and/or breaker angle varies along the shore may be described as a non-uniform alongshore current.

The author's investigation involved a laboratory study of a non-uniform alongshore current system generated by an alongshore gradient of breaker height with the wave crests parallel to the beach. A previous paper (6) described the experimental arrangements and techniques; presented the general results of a typical test; and treated some aspects involving the calculation of the wave set-up. This paper presents experimental results for various deep water wave heights, H_o , and two wave periods, T , and describes a simple method for calculating the wave generated current for the situation where the driving force causing the current is created solely by the alongshore gradient of breaker height.

* Department of Civil Engineering, University of Queensland, St. Lucia, Australia

2. Laboratory Experimental Arrangements

The layout of the 12.5 m by 6.6 m outdoor test basin and the measurement methods used were described in a previous paper (6) to which the reader is referred for a more complete description. The experimental arrangement involved the generation of a non-uniform alongshore current by wave diffraction behind an offshore breakwater in a three dimensional fixed bed laboratory model (Figure 1). Waves approached with crests parallel both to the breakwater and the exposed portion of the 1 in 10 concrete beach while the beach in the sheltered area was curved so that it was parallel to the crests of the diffracted waves. Waves thus broke at all times parallel to the beach. The breakwater itself was located at a distance of 3.05 m from the still water line in the exposed area, while the constant offshore water depth at the head of the breakwater was 0.2 m.

Wave heights were recorded using capacitative wave probes and a twin channel pen recorder; wave set-up was measured using piezometer tappings in the beach and a multtube manometer; and current velocities and circulation patterns were obtained from the analysis of movie film records of the paths of small almost neutrally buoyant floats together with some direct measurements with a modified total head tube device (see section 3.1).

3. Results of Laboratory Investigation

3.1 Basic Characteristics of Non-uniform Alongshore Current System

The characteristics of the current system generated in the test basin were described in a previous paper (6). In that description the results of one test only for a specific H_o and T were considered. To assist in the understanding of the results presented in this paper a brief description of the current system will be given first. Referring to figure 2 it can be seen that as a consequence of the diffraction of the waves by the offshore breakwater, the surf zone is wide in the exposed area where the waves are large while it is narrow within the sheltered area where the waves are of necessity very much smaller. An alongshore gradient of breaker height is thus present and this results in an alongshore gradient of wave set-up since the latter is generally proportional to the breaker height in shallow water.

Now the wave set-up itself is maintained by the onshore thrust created by the change in momentum as the breaking waves are dissipated within the surf zone. However there is no such opposing thrust in the longitudinal direction to balance the alongshore gradient in the mean water level resulting from the alongshore variation in wave set-up. The result is that an alongshore current flows from the surf zone of the exposed area into the sheltered area. Since the geometry of the system is a closed one the alongshore current becomes a circulatory eddy. Referring to figure 2 it is seen that the entire circulation is contained inside the point where the exposed area breaker height is a maximum, i.e. inside of the first interference maximum of the diffraction pattern.* Moreover the seaward limit of the current is initially defined by the location of the plunge point in the exposed area since this represents the point in the onshore-offshore direction where wave set-up commences. Between the point of maximum breaker height and the geometric shadow of the breakwater there is a zone of spatially varied flow where the alongshore current discharge increases as it travels towards the sheltered area since water flows inshore through the breakers from further

* A series of secondary circulation systems is set up in the exposed area where the alternating interference maxima and minima provide the necessary alongshore gradients in energy levels to produce rip currents. The first such rip current occurred within the test basin but as it was affected by the presence of the model sidewall (especially for 1.5 second waves) it was not studied in detail.

offshore. The current discharge itself attains a maximum value at the geometric shadow of the breakwater.

Within the sheltered area the current becomes too large to remain within the rapidly narrowing surf zone and so flows increasingly outside the breaker line until it is eventually completely removed from the surf zone. It is deflected by the stagnation eddy at the corner where the breakwater intersects the curved beach. The return circuit is then completed as the current flows along the shoreward face of the breakwater before turning shoreward at the head of the breakwater to flow back into the surf zone in the inflow region. Inside the primary wave generated current the initially motionless fluid is set in motion by the current and moves as a slow induced eddy within the main current system.

The driving force for the current system appears to be essentially the increase in head created by the breaking waves in the inflow region. Indeed the current system can be visualized as being powered by a "pump" located in the inflow region drawing water in from the offshore zone and discharging it as a high velocity "jet" parallel to the beach. The "jet" is then deflected by the curved beach and breakwater so that it flows back into the "pump" inlet, offshore of the inflow region. Diffusion of momentum offshore creates the induced eddy inside the primary current circulation.

Observations of horizontal velocity profiles of the current, made from photographs of surface floats, indicate that the surface velocity profile is approximately parabolic in shape with a rather well defined offshore boundary between the primary alongshore wave generated current and the induced eddy inside it (figure 3). Measurement of the vertical velocity profile of the alongshore current is much more difficult on account of the very shallow depths in the surf zone and the unsteady nature of the wave orbital motion superimposed at right angles to it. Figure 4 shows one such profile measured along the line of the geometric shadow of the breakwater using a small pitot tube device with two total head tubes, one pointing upstream and the other downstream. Figure 4 includes surface float data from figure 3 which are found to be consistent with the sub-surface measurements resulting in the velocity contours as shown. The maximum velocity occurs within the surf zone, just below the wave trough elevation. Integration of the velocity with respect to depth indicated that the actual current discharge (or mean velocity) is in fact about 50% greater than that calculated from surface float velocities alone. Consideration of the isovel pattern, together with visual observation of the uprush-backwash cycle in the test basin shows that there is spiral secondary flow superimposed upon the primary alongshore current similar to the helicoidal flow observed in the field by Eliot (8) for alongshore currents.

3.2 Influence of Variations in Wave Height and Period upon the Current System

The effect of variations in input wave conditions, upon the wave generated current system was obtained from the results of two series of tests, one made with a wave period of 1.0 seconds, the other with a period of 1.5 seconds. Each test series consisted of four tests with different deepwater wave heights. Two parallel series of tests were also made in which the sheltered area of the test basin was blocked off so as to give two dimensional conditions in the exposed area.

The experimental results indicate that there is a general overall similarity of the current circulation system for all H_o and T. Variations in detail do occur but the geometrical form of the beach and breakwater determine the overall form of the current system. For instance when breaker height H_b and wave set-up at the still water line \bar{H}_s are made nondimensional in terms of H_b^* and \bar{H}_s^* , their equivalent two dimensional values for the same H_o and T, general similarity is found for each period (figure 5). Different wave periods which correspond to different

deep water wave lengths, L_0 , cause some differences in the alongshore gradients of breaker height and wave set-up. Specifically, in the region between the maximum wave height in the exposed area and the geometric shadow of the breakwater, the alongshore gradient of dimensionless wave set-up is greater for 1.0 second period waves than for 1.5 second waves. This difference is in agreement with diffraction theory. The alongshore dimensionless breaker height also varies locally in two regions with the deep water wave height. This effect, which occurs in the sheltered area in the vicinity of the stagnation eddy and in the exposed area outside the primary current circulation system, is caused by interaction between the waves and the wave generated currents.

Similarity of the alongshore velocity profiles may be considered from two points of view. The first is to express the velocity profiles in nondimensional parameters based upon the breaking wave conditions which should relate the velocities to those quantities which most directly influence them. Alternatively the alongshore current velocities can be related to the incident or deepwater wave conditions and geometric factors which determine the overall characteristics of the nearshore current system.

Consideration of theoretical investigations for uniform alongshore currents such as that of James (9) suggests that an appropriate set of dimensionless parameters to represent this data would be the following:

$$\frac{v}{\sqrt{gd_b^*}} ; \frac{x}{d_b^*} ; T \sqrt{\frac{g}{d_b^*}}$$

where v is the alongshore velocity at distance x from the still water line;

$d = \bar{\eta} + h$ is the mean water depth;

h is the still water depth.

These parameters are used to plot dimensionless velocity profiles along the geometric shadow for wave periods of 1.0 and 1.5 seconds as shown on figure 6. There is considerable scatter in the data points but it does appear that the dimensionless velocity and distance parameters are satisfactory. However it is evident that the 1.0 second period tests do not show the same consistent variation with the third parameter as shown by the 1.5 second tests. Moreover the magnitudes of this latter parameter are inconsistent for the two wave periods. Analogy between James' theory and theory for non-uniform alongshore currents (e.g. Komar (3)) shows that the velocity profiles could also be affected by the following dimensionless quantities:

$$\frac{dH_b}{dy} ; \gamma = \frac{H_b}{d_b} ; N ; C_f ; \tan \alpha$$

Of these, the bottom slope $\tan \alpha$ was constant in these tests. The bottom friction coefficient C_f is a complex function of the wave orbital velocity and the alongshore velocity. As indicated in section 4.3, bottom friction effects are relatively small in this situation. The factors upon which the lateral mixing coefficient N depends are not yet clear and its exact magnitude remains uncertain. The alongshore gradient in breaker height will only affect the alongshore velocity significantly if bottom friction is important. Otherwise it is the dimensionless difference in alongshore breaker height $\Delta H_b / H_b^*$ which is important and this is the same for both wave periods. This leaves only the breaker index γ as an alternative relevant third parameter. However, while there is some evidence of better agreement between the two series of tests when the equivalent two dimensional breaker index γ^* is considered as the third parameter on figure 6, complete consistency is impossible since γ^* varies in opposite senses for the two wave periods.

Figure 7 shows the dimensionless maximum alongshore velocity as a function of the alongshore distance y for each wave period. This clearly indicates that the magnitude of the velocity is influenced by quantities other than $\sqrt{gd_b^k}$ but as before it is not possible to deduce a simple dependence upon any one of the parameters previously considered which applies to both wave periods.

Considering the alternative of relating the current velocity to the deep water wave conditions it is quite evident that the alongshore current velocity increases with wave height. Consequently the maximum velocity v_m was plotted as a function of H_o for each location along the shoreline. A simple picture emerged in which $v_m = B(t)H_o$ where $B(t)$ varied consistently along the shoreline. Figure 8a shows the plot of v_m versus H_o for the profile at the geometric shadow. Similar plots were obtained at the other locations with relatively few discordant points. The magnitude of $B(t)$ has been plotted as a function of the alongshore distance in figure 8b. This figure suggests that, apart from the slight variation with wave period of the location of the point where the current commences, which is a result of the effect of the wave length upon the diffraction process, the wave period does not enter the current velocity similarity parameter. Thus the alongshore current velocity is apparently determined by the deepwater incident wave height H_o and the geometric characteristics of the system. As the latter were not varied in these tests the relevant variables can only be inferred at this stage. The relevant parameters could be the following:

$$\frac{v_m}{\sqrt{gd_i}} = B \left(\frac{H_o}{X} \right)$$

where $B = f \left(\frac{Y}{X}, \frac{d_i}{X}, \tan \alpha \right);$

d_i is the incident water depth at the breakwater;

and X is the distance between breakwater and still water line.

3.3 Interaction between Alongshore Current and Wave Set-up

As previously mentioned the alongshore current modifies the breaker heights in certain regions. The wave set-up is also modified by changes in the mean water level created by the current system. In figure 9 the wave set-up at still water level, \bar{n}_s , is plotted as a function of the corresponding breaker height measured in the three dimensional basin, for each of the four tests with 1.0 second wave period. For comparison the equivalent relation between \bar{n}_s and H_b derived from the two dimensional tests is shown on each plot. It can be clearly seen that in the three dimensional case the wave set-up \bar{n}_s is relatively greater than its two dimensional value for the corresponding breaker height and that this discrepancy increases with increasing deep water wave height H_o . Since the current velocity also increases with H_o (figure 8) it would appear that \bar{n}_s increases as the current velocity increases. The tests with 1.5 second period waves indicate a similar result. In figure 10, \bar{n}_s is plotted on a very much magnified scale as a function of the distance along the still water line for one of the tests. Also shown on figure 10 is the equivalent two dimensional wave set-up \bar{n}_s^* corresponding to the observed alongshore variation in breaker height. \bar{n}_s^* is plotted downwards from the corresponding three dimensional value of \bar{n}_s and, except at two points, the two dimensional value is generally about 10 to 15% smaller than the three dimensional value.

The following specific characteristics of the alongshore variation of wave set-up may be discerned from figures 9 and 10:

- (i) The wave set-up has its maximum value in the region within the exposed area outside the primary alongshore current system where it is essentially independent of the breaker height (see also figure 5). This represents the effect of the alongshore feeder currents to the rip current, which produce a stagnation condition on the shore at the point where the rip current flows seaward through the breaker zone.
- (ii) The two dimensional wave set-up is greater than the three dimensional set-up at points where there is inflow into the surf zone and alongshore outflow in both directions with a consequent reduction in the magnitude of the backwash.
- (iii) The maximum discrepancy between the three and two dimensional wave set-up generally occurs at or near the geometric shadow line defining the boundary between exposed and sheltered areas. This corresponds to the region where the alongshore velocity attains its maximum value.
- (iv) The minimum value of wave set-up occurs within the sheltered area but not right at the corner on account of refraction of the waves by the current which increases breaker heights within the stagnation eddy but reduces them further upstream.

The explanation for the difference between the three and two dimensional wave set-ups is found in three separate factors. These are breakpoint set-up, $\bar{\eta}_b$; superelevation caused by normal acceleration, $\bar{\eta}_c$; and alongshore translation of the uprush-backwash cycle, $\bar{\eta}_d$. Hence the wave set-up at the still water line at position y within the region influenced by the primary alongshore current is given as follows:

$$\bar{\eta}_s = \bar{\eta}_s^* + \bar{\eta}_b + \bar{\eta}_c + \bar{\eta}_d$$

Breakpoint set-up $\bar{\eta}_b$

In the three dimensional case expansion of the diffracted wave crests behind the breakwater causes a reduction in radiation stress and a consequent increase in mean water level. This results in a breakpoint set-up $\bar{\eta}_b$ in the sheltered area of the order of 1 mm for the particular test shown on figure 10. This factor accounts for about half the observed discrepancy in the stagnation region. In the exposed area there is a breakpoint set-down of similar order of magnitude.

Superelevation caused by normal acceleration $\bar{\eta}_c$

The alongshore current is deflected by the beach and the resulting normal acceleration results in a superelevation of the water surface on the beach. This has been calculated using the relationship

$$\bar{\eta}_c = \sum \frac{v^2}{gr} \Delta r$$

where r is the radius of curvature of the flow streamlines.

The value of $\bar{\eta}_c$ has been plotted on figure 12 upwards from the breakpoint set-up level. It is found that all the three dimensional wave set-up is now accounted for within the stagnation eddy region. With regard to the rip current in the exposed area, calculation of the stagnation velocity of the alongshore feeder currents confirms the previously quoted explanation for the increased wave set-up in this region.

Alongshore translation of uprush-backwash cycle $\bar{\eta}_d$

Visual observation in the test basin suggested that the process referred to earlier in which a helicoidal secondary motion is superimposed upon the primary alongshore current also provides the explanation for the remaining component of the three dimensional wave set-up in the vicinity of the geometric shadow of the breakwater where the alongshore current has its maximum value. Referring to

figure 11 it can be seen that the wave set-up at a point on the beach is in fact determined by waves breaking further upstream along the beach since the alongshore current translates the wave uprush-backwash cycle along the beach. Thus the magnitude of the wave set-up at a point C within the alongshore current depends upon the height of the breaking waves between points A and B upstream of it; and not upon the breaker height at point D on the same profile as point C.

The actual magnitude of the increase in $\bar{\eta}_s$ at point C will depend upon both the velocity of the alongshore current between points A and C and the alongshore gradient of breaker height between points A and B. A simple estimate of this effect was calculated using the observed variation of mean alongshore velocity V and the alongshore variation of the gradient of $\bar{\eta}_s^*$ calculated from the observed breaker heights. Assuming that the mean alongshore displacement distance Δy is equal to the distance travelled by the mean alongshore current during one wave period T, the increase in wave set-up, $\bar{\eta}_d$, at a certain point is given by the following expression:

$$\bar{\eta}_d = VT \frac{d(\bar{\eta}_s^*)}{dy}$$

where the magnitudes of $\frac{d(\bar{\eta}_s^*)}{dy}$ and V are those at a point located a distance equal to $\Delta y = VT$ upstream of the point under consideration.

The results of this calculation are found to give values of $\bar{\eta}_d$ which agree to within 0.3 to 0.5 mm of the observed values. The agreement is particularly good in the inflow zone in the exposed area but not so good in the sheltered area where the current leaves the surf zone. It is however considered adequate for confirmation of this explanation for the influence of the current upon the magnitude of $\bar{\eta}_s$ in the three dimensional case. The remaining small discrepancy may be explicable by the fact that the diffracted wave crests are not exact circular arcs. Consequently the breaker angle may not be exactly zero everywhere along the beach.

4. Computation of Alongshore Current

4.1 General Scheme of Computation

The calculation of the alongshore current from the alongshore gradient of wave set-up has not been found to be easy for a number of reasons. For instance, apart from the nonlinear interaction effects between the current and the wave set-up, there are the problems of defining the seaward extent of the current; the extent of the inflow region where water is being fed into the surf zone from offshore; the point where the current leaves the surf zone and the magnitude of the bottom friction and lateral mixing effects.

The computation process may be considered in four basic stages. These are as follows:

- (i) Determination of the alongshore gradient of breaker height and the location of the break point;
- (ii) Determination of the wave set-up resulting from the alongshore gradient of breaker height;
- (iii) Determination of the wave generated current from the previously determined alongshore gradient of wave set-up;
- (iv) Adjustment of the first estimate of the wave generated current for the effects of interaction between the current and the surf zone conditions.

In a previous paper (6) the author has described how it is possible to determine the location of the breakpoint and the alongshore breaker height gradient

using a graphical combination of 1st order diffraction and shoaling theory together with empirical wave breaking data correlated by Goda (10). The results of this computation were generally promising. However to simplify the treatment of the subsequent stages of the computation process the work described in this paper takes the observed break point and alongshore variation of breaker heights as its starting point.

4.2 Wave Set-up

With regard to the determination of the wave set-up this can be approached from two viewpoints. Firstly a purely empirical approach can be adopted. For instance, the parallel series of two dimensional tests yielded the empirical relationships;

$$\bar{\eta}_s = 0.303 H_b \left[\frac{H_o}{L_o} \right]^{0.12} \quad 1.$$

$$\bar{\eta}_m = 0.288 H_b \quad 2.$$

where $\bar{\eta}_s$ is the wave set-up at the still water line

and $\bar{\eta}_m$ is the maximum wave set-up.

Such empirical relationships derived from this study have the drawback that they allow, neither for the influence of the geometry of the particular two dimensional system in which the measurements were made, nor for scale effects. An alternative approach is to compute the wave set-up using the radiation stress theory of Longuet-Higgins and Stewart as applied by Bowen et al (11), assuming that conditions at the breakpoint and within the surf zone can be represented by the shallow water approximations. On this basis Bowen et al have shown that the mean water level gradient normal to the shore is given by the following expression:

$$\frac{d\bar{\eta}}{dx} = - \frac{1}{1 + 8/3\gamma^2} \cdot \frac{dh}{dx} \quad 3.$$

where $\frac{dh}{dx} = \tan \alpha$ is the bottom slope.

Wave set-down at the breakpoint, assuming the same approximations, is given by:

$$\bar{\eta}_b = - \frac{1}{16} \gamma H_b \quad 4.$$

Simple geometry then permits the derivation of relationships for $\bar{\eta}_s$ and $\bar{\eta}_m$ as functions of γ and H_b in the manner presented by several authors (12, 13 and 14). All these authors assume spilling breakers. Plunging breakers have been treated in a similar manner by Swart (15) and Gourlay (6). In this case an additional parameter is involved, either an energy dissipation factor as in Swart's treatment or the breaker plunge distance x_p in Gourlay's treatment.

For the present study it has been found expedient to adopt slightly modified forms of these empirical relationships in which the wave set-up is referred to the mean water level at the breakpoint rather than the deep water mean water level. This involves neglect of the break point set-down (equation 4) which in the case under consideration varies in the alongshore direction becoming positive in the sheltered area (see section 3.3). In passing it should also be noted that equation 4 generally overestimates the observed wave set-down by a factor of 2 to 3. As the set-down is at least an order of magnitude smaller than the wave set-up, its inclusion at this stage in the calculation of the latter is questionable.

Taking account of the above points the relevant equations for the computation of wave set-up assuming shallow water conditions within the surf zone may be summarized as follows:

$$\bar{\eta}_s^1 = \frac{3}{8} \gamma \frac{(1 - C \gamma \tan \alpha)}{1 + 3\gamma^2/8} H_b \quad 5.$$

$$\bar{\eta}_m^1 = \frac{3}{8} \gamma (1 - C \gamma \tan \alpha) H_b \quad 6.$$

where $C = \frac{x_p}{H_b}$
 = 0 for spilling breakers
 = 2 to 4 for plunging breakers

and $\bar{\eta}_s^1$ and $\bar{\eta}_m^1$ represent wave set-ups measured relative to mean water level at the breakpoint.

The author has previously shown (figure 13 of reference 6) that equation 5 gives reasonable estimates of $\bar{\eta}_s^1$ as measured in the two dimensional tests of this investigation, having regard to the general uncertainty as to what factors determine the magnitude of the dimensionless plunge distance C . Equation 6 has been found to behave similarly with respect to $\bar{\eta}_m^1$.

When plunging breakers are considered it is necessary to be able to determine the depth h_p at the plunge point. Simple geometry gives the following result compatible with equations 5 and 6.

$$h_p = \frac{(1 - C \gamma \tan \alpha)}{\gamma} H_b \quad 7.$$

The analogous directly derived experimental result compatible with equations 1 and 2 is:

$$h_p = 2.55 \bar{\eta}_s = 0.773 H_b \left[\frac{H_0}{L_0} \right]^{0.12} \quad 8.$$

4.3 Mean Velocity of the Alongshore Current

The following observations of the characteristics of the non-uniform alongshore current have been used in formulating a simple analytical expression for computing the maximum mean velocity of the current.

- (i) Inflow into the alongshore current ceases at the geometric shadow line. Hence discharge Q and mean velocity V are assumed to have attained their maximum values at this point.
- (ii) The seaward limit of the current at this point corresponds to the distance x_{c1} from the still water line to the plunge point of the largest breakers in the exposed area.
- (iii) The landward limit of the current occurs at the point where the onshore-offshore gradient of mean water level intersects the beach, i.e. at the point where the wave set-up equals $\bar{\eta}_m$ located at a distance x_s from the still water line.

The differential equation of motion in the alongshore direction is written as follows:

$$\frac{dS_{yy}}{dy} + \rho g(\bar{\eta} + h) \frac{d\bar{\eta}}{dy} + \rho \frac{d}{dy} [v^2(\bar{\eta} + h)] + \tau_b + \tau_l = 0 \quad 9.$$

where S_{yy} is the alongshore component of the "radiation stress";

τ_b and τ_l are the shear stresses due to bottom friction and lateral mixing respectively.

For a simple engineering solution we will adopt a control volume type of analysis initially neglecting the effects of bottom friction and lateral mixing,

$$\tau_b \text{ and } \tau_l \rightarrow 0$$

In the alongshore direction (y) the control volume is assumed to be bounded in the upstream direction at the point where the alongshore current velocity V is zero and H_b has its maximum value. The downstream end of the control volume is at the geometric shadow where both velocity and discharge have attained their maximum values. The offshore limit of the control volume in the x direction is assumed to be equal to x_{cl} as noted above. The form of the water surface at either end of the control volume is as indicated in figure 12.

Application of the momentum principle, i.e., the integral form of equation 9, to the flow of the alongshore current into and out of this control volume in the y direction gives the following expression:

$$\rho A_2 V_2^2 = P_1 + S_1 - (P_2 + S_2) \quad 10.$$

where A is the cross sectional area of flow;

P is the integrated thrust due to hydrostatic pressure

S is the integrated thrust due to radiation stress;

V is the mean velocity of flow through a given cross section;

ρ is the fluid density

and subscripts 1 and 2 refer to upstream and downstream locations respectively.

Using the shallow water approximation for S_{yy} ,

$$S_{yy} = \frac{1}{16} \rho g \gamma^2 (\bar{n} + h)^2 \quad 11.$$

together with equation 3, simple geometry and integration lead to the following relations:

$$P_1 + S_1 = \frac{\rho g}{6 \tan \alpha} (1 + \frac{\gamma^2}{8}) (h_{p1}^2 + \bar{n}_{m1} h_{p1}^2) \quad 12.$$

$$P_2 + S_2 = \frac{\rho g}{6 \tan \alpha} (1 + \frac{\gamma^2}{8}) (h_{p1}^3 + \frac{64\bar{n}_m^3}{9\gamma^4}) \quad 13.$$

$$A_2 = \frac{1}{2 \tan \alpha} (h_{p1}^2 + \frac{8\bar{n}_m^2}{3\gamma^2}) \quad 14.$$

In obtaining equation 13 for $P_2 + S_2$ it has been assumed that the ratio between wave height and water depth, γ , is the same outside of the plunge point as inside of it. While this assumption is of course not valid, the simplification of the form of the resulting expression for $P_2 + S_2$ is considered to more than offset the resulting relatively small underestimation of the final value of V .

Substitution into equation 10 yields the result

$$V_2 = \sqrt{\frac{g}{3} (1 + \frac{\gamma^2}{8}) \frac{h_{p1}^2 \bar{n}_{m1}}{h_{p1}^2 + \frac{8\bar{n}_m^2}{3\gamma^2}} - \frac{64\bar{n}_m^3}{9\gamma^4}} \quad 15.$$

Further simplification is dependent upon the following decisions:

- (i) The choice between equations 8 and 2 or equations 7 and 6 for expressing h_p and \bar{H}_m in terms of the incident wave conditions.
- (ii) The specification of the alongshore gradient of \bar{H}_m or as a consequence of the substitutions for \bar{H}_m referred to in (i) above, the specification of the alongshore gradient of breaker height.

With regard to (i) equations 8 and 2 express h_p and \bar{H}_m in terms of H_b and H_o/L_o with the bottom slope $\tan \alpha$ implicit in the constants while equations 7 and 6 express them in terms of H_b , γ , C and $\tan \alpha$. In the latter case γ is known to be a function of H_o/L_o and $\tan \alpha$ (10). Since equation 15 already includes the breaker index γ , the substitution of the theoretical equations 7 and 6 will be adopted as most likely to produce a simple consistent result.

As to (ii) this is determined by the system geometry and is of course the result of the combined diffraction - shoaling process behind the breakwater. Consideration of figure 5 suggests that it will be reasonable in the first instance to assume the following relationship for the alongshore change in breaker height.

$$H_{b1} = 2 H_{b2} = H_b^* \quad 16.$$

When the relevant substitutions based upon the above considerations are made in equation 15 the latter becomes

$$\frac{V}{\sqrt{gH_b^*}} = \sqrt{\frac{7}{64} \gamma \left(1 + \frac{\gamma^2}{8}\right) \frac{(1 - C \gamma \tan \alpha)}{1 + 3 \gamma^2 / 32}} \quad 17.$$

Equation 17 is compared with experimental values on figure 13.

The general result is similar to that for the two dimensional wave set-up (6) in that most of the experimental values lie within the scatter resulting from the possible variation of the parameter C .

A similar substitution in equation 14 yields

$$\frac{A}{H_b^{*2}} = \frac{(1 + 3\gamma^2/32)(1 - C \gamma \tan \alpha)^2}{2 \gamma^2 \tan \alpha} \quad 18.$$

and combination of equations 17 and 18 leads to an expression for the discharge of the alongshore current of the following form:

$$\frac{0}{g H_b^*} \gamma_2 = f(\gamma, C, \tan \alpha) \quad 19.$$

$$\text{where } \gamma = f\left(\frac{H_o}{L_o}, \tan \alpha\right)$$

$$C = f(\tan \alpha, ?) \quad \text{- see Galvin (16).}$$

The comparatively good agreement of equation 17 with experimental observations indicates that the assumption of negligible bottom friction is reasonable. It is however desirable to check this assumption more positively by incorporating the bottom friction force T into the original momentum analysis. Equation 10 now becomes

$$\rho A_2 V_2^2 = P_1 + S_1 - (P_2 + S_2) - T \quad 20.$$

T can be most conveniently evaluated using the non-linear expression for bed shear stress proposed by Jonsson et al (17),

$$\tau_b = f_s \frac{1}{2} \rho V^2$$

where $f_s = f (f_c, f_w \text{ and } \frac{u_{bm}}{V})$

f_c is the current friction factor which is estimated by the usual rough boundary logarithmic formula;

f_w is the wave friction factor which is estimated using the equations of either Jonsson (18) or Kamphuis (19);

u_{bm} is the maximum value of the wave orbital velocity within the surf zone.

Assuming a constant value of f_s determined by average values of f_c , f_w and u_{bm}/V together with a linear variation of mean velocity V with alongshore distance y , within the inflow region, the friction force is given by

$$T = \frac{\rho f_s Y}{6 \tan \alpha} [h_{p1} + \frac{1}{2} (\bar{H}_{m1} + \bar{H}_{m2})] V^2 \quad 21.$$

where Y is the alongshore length of the control volume.

Using the same substitutions as were used to obtain equation 17 from equation 15 the following expression including the effect of bottom friction is obtained:

$$\frac{V}{\sqrt{gH_b^*}} = \sqrt{\frac{\frac{7}{64} \frac{Y}{8} (1 + \frac{Y^2}{8}) (1 - C\gamma \tan \alpha)}{1 + \frac{3Y^2}{32} + \frac{f_s Y (1 + 9Y^2/32)}{3(1 - C\gamma \tan \alpha)} \cdot \frac{Y}{H_b^*}}} \quad 22.$$

It is doubtful whether the use of an equation of the complexity of equation 22 is warranted. For instance taking a specific test and substituting actual observed wave conditions and surf zone geometry into equation 20 using equations 12, 13, 14 and 21 enables the effect of bottom friction upon the magnitude of V to be estimated.

For example, for the test with the following conditions

$$\begin{aligned} T &= 1.0 \text{ s} ; & H_0 &= 69 \text{ mm} ; & H_b^* &= 77 \text{ mm} ; \\ h_{p1} &= 44 \text{ mm} ; & \bar{H}_{m1} &= 22 \text{ mm} ; & \bar{H}_{m2} &= 11 \text{ mm} ; \\ Y &= 1.2 \text{ m} ; & \gamma &= 1.0 ; & \tan \alpha &= 0.1 ; \\ f_s &= 0.025. \end{aligned}$$

the observed value of V was 0.25 m/s.

Neglecting the friction force, V was 0.23 m/s.

and allowing for the friction force, V was 0.21 m/s.

4.4 Further Aspects of Non-uniform Alongshore Current Computations

The planning of the author's experimental work was directed to obtaining a situation where the driving force for the alongshore current resulted solely from an alongshore gradient in breaker height. This represents one limiting case for alongshore currents, the completely non-uniform alongshore current. At the

opposite end of the spectrum lies the uniform alongshore current whose driving force results solely from waves of uniform height breaking at an angle to an infinitely long plane beach. The author's situation represents a current system which is very definitely limited in size and which in fact results in a closed circulation system. The uniform alongshore current on the other hand is ideally of infinite length and open ended in nature.

Once the above contrasts are appreciated it is clear that there may be significant differences in the formulation of theoretical models to allow for the effects of alongshore gradients of breaker height upon the velocity of the alongshore current. In the situation studied by the author the alongshore current is only related to surf zone characteristics within the inflow region where the flow is highly non-uniform and the current discharge is increasing in the alongshore direction. Thus the consideration of the convective acceleration term and variable surf zone width is essential but bottom friction is relatively insignificant. On the other hand if the problem is approached as one where the alongshore gradient of breaker height is modifying the alongshore current produced by waves breaking at an angle to the shoreline, then the bottom friction term is almost certainly more important than the convective acceleration term and the variation in surf zone width with breaker height can be neglected. This latter situation is the one envisaged by Bakker (20) and Komar (3) in their approaches to non-uniform alongshore currents. The differences between the two approaches arise essentially from the assumption of either a large or a small alongshore gradient of breaker height.

The simple methods for computation of non-uniform alongshore currents presented in this paper are subject to the following limitations:

- (i) The breaker angle has been assumed to be negligible.
- (ii) Both the offshore boundary of the current and the alongshore gradient of breaker height have been determined from experimental observations for the particular system considered.
- (iii) The downstream component of the thrust on the control volume due to radiation stress has been overestimated. This results in an underestimation of the alongshore current velocity. However as the magnitude of this error is of the same order but less than the magnitude of the bottom friction force, its overall effect is negligible.
- (iv) The following factors have been ignored or assumed to be negligible:
 - wave set-down or set-up at breakpoint;
 - lateral mixing and the resulting shear stress at the offshore boundary of the control volume as well as the effect of non-uniform velocity distribution upon the momentum thrust;
 - interaction between the alongshore current and the wave surf zone parameters.
- (v) Both the breaker index γ and the dimensionless plunge distance C are based upon laboratory experimental data without any adequate supporting theory to relate them to the offshore wave conditions.

5. Conclusion

For an alongshore current system resulting solely from an alongshore gradient of breaker height produced by diffraction behind an offshore breakwater,

it has been found that the basic current pattern is imposed by the system geometry and that there is a general similarity of alongshore breaker height and wave set-up gradients in terms of their equivalent two dimensional values.

For a given geometry the alongshore current velocity is primarily determined by the deepwater wave height. The wave period appears to have only a secondary effect upon the alongshore current system. The relationship between the current velocity and surf zone parameters has not been clearly established.

The alongshore variation of wave set-up may be considerably influenced by the alongshore current and may be increased above its two dimensional value by the effects of break point set-up, superelevation caused by normal acceleration and alongshore translation of the uprush-backwash cycle.

A simple theoretical analysis has shown that the alongshore current velocity at the point where maximum discharge is attained can be calculated as a function of the equivalent two dimensional breaker height, the breaker constants γ and C and the bottom slope. Bottom friction can be allowed for but has a comparatively small effect in the situation considered.

6. References

1. Galvin, C.J. Longshore current velocity : A review of theory and data. *Reviews of Geophysics* Vol. 5, No.3. Aug. 1967, pp 287-304.
2. Longuet-Higgins, M.S. Recent progress in the study of longshore currents. *Waves on Beaches and Resulting Sediment Transport - R.E. Meyer (Editor)*. Academic Press, New York, 1972, pp 203-248.
3. Komar, P.D. Nearshore currents : Generation by oblique incident waves and longshore variations in breaker height. *Nearshore Sediment Dynamics and Sedimentation - J. Hails and A. Carr (Editors)*. Wiley, London, 1975, pp 17-45.
4. Bowen, A.J. Rip currents 1. Theoretical Investigations. *Jour. Geophys. Res.* Vol. 74, No.23, Oct.20, 1969. pp 5467-5478.
5. Bowen, A.J. and Imman, D.L. Rip currents 2. Laboratory and field observations. *Jour. Geophys. Res.* Vol. 74, No.23, Oct. 20, 1969, pp 5479-5490.
6. Gourlay, M.R. Wave set-up and wave generated currents in the lee of a breakwater or headland. *Procs. 14th Int. Conf. on Coastal Engineering*, Copenhagen, 1974, Vol. III, pp 1976-1995.
7. Gourlay, M.R. Wave generated currents - some observations made in fixed bed hydraulic models. *Univ. of Qld, Dept. of Civil Engineering Bull.* No.7, Nov. 1965.
8. Eliot, J. The persistance of rip current patterns on sandy beaches. *Engineering Dynamics of the Coastal Zone*. I.E. Aust., 1st Australian Conference on Coastal Engineering, Sydney, May 1973, pp 29-34.
9. James, I.D. A non-linear theory of longshore currents *Estuarine and Coastal Marine Science* Vo. 2, 1974, pp 235-249.
10. Goda, Y. A synthesis of breaker indices *Trans. J. S.C.E.* Vol. 2, Part 2, 1970, pp 227-230.

11. Bowen, A.J., Imman, D.L. and Simmons, V.P.
Wave "set-down" and set up.
Jour. Geophys. Res. Vol. 73, No.8, April 15, 1968, pp 2569-2577.
12. Bakker, W.T. Littoral drift in the surf zone.
Rijkswaterstaat, Directorate for Water Management and Hydraulic Research, Dept. of Coastal Research, The Hague, Study Report WK70-16, 1970.
13. Tait, R.J. Wave set-up on coral reefs.
Jour. Geophys. Res. Vol. 77, 1972, pp 2207-2211.
14. Battjes, J.A. Computation of set-up, longshore currents, run-up and overtopping due to wind-generated waves.
Delft Univ. of Technology, Dept. Civ. Engng. Comm. on Hydraulics. Report No. 74-2, 244 p, 1974.
15. Swart, D.H. Offshore sediment transport and equilibrium beach profiles.
Delft Hydraulics Laboratory. Publication No. 131, 1974.
16. Galvin, C.J. Breaker travel and choice of design wave height.
Procs. ASCE, Vol. 95, No. WW2, May 1969, pp 175-200.
17. Jonsson, I.G., Skovgaard, O. and Jacobsen, T.S.
Computation of longshore currents.
Procs. 14th Int. Conf. on Coastal Engineering, Copenhagen, 1974, Vol II, pp 699-714.
18. Jonsson, I.G. The wave friction factor revisited.
Tech. Univ. Denmark., Inst. Hydrodyn and Hydraulic Engng.
Prog. Rep. 37. Dec. 1974, pp 3-8.
19. Kamphuis, J.W. Friction factor under oscillatory waves.
Procs. ASCE, Vol. 101, No. WW2, May 1975, pp 135-144.
20. Bakker, W.T. The influence of longshore variation of the wave height on the littoral drift.
Rijkswaterstaat, Directorate for Water Management and Hydraulic Research, Dept. for Coastal Research, The Hague. Study Report WK 71-19, 1971.



Figure 1. General View of Test Basin

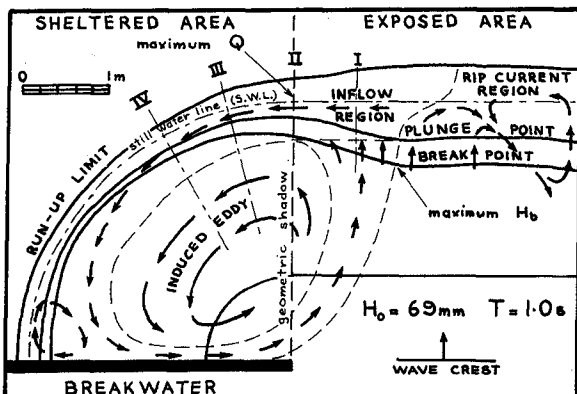


Figure 2 WAVE GENERATED CURRENT SYSTEM

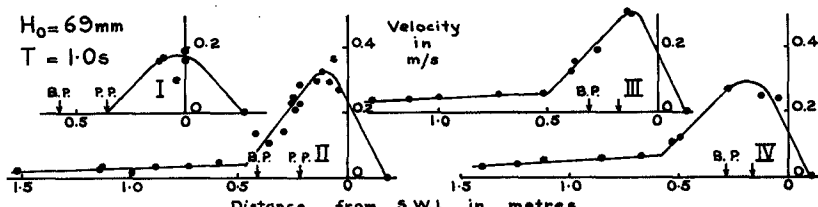


Figure 3 SURFACE VELOCITY PROFILES

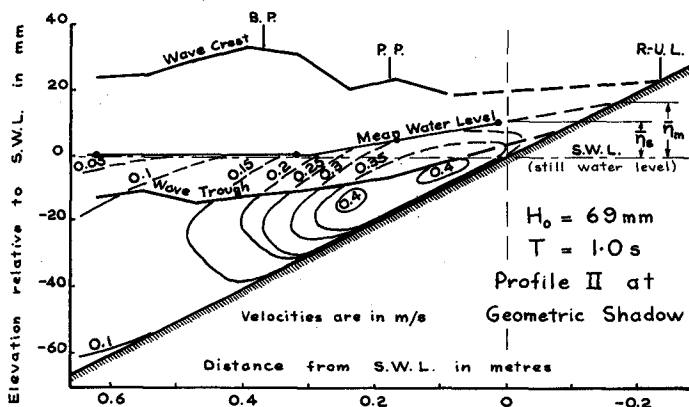


Figure 4 VERTICAL VELOCITY PROFILE

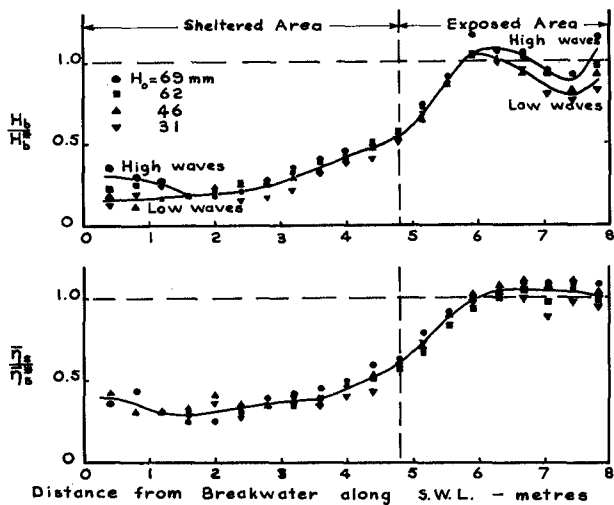
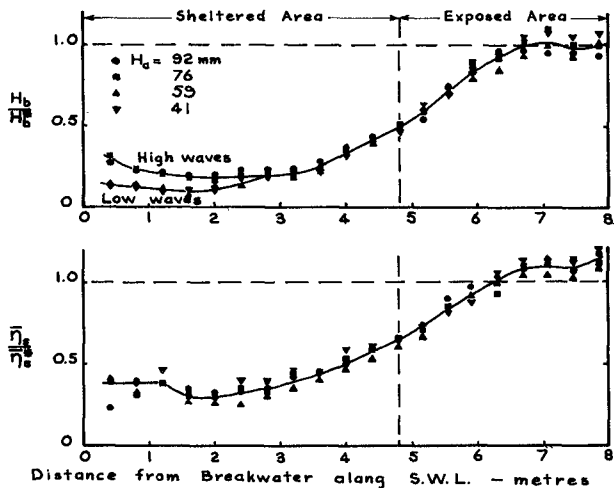
(a) $T = 1.0$ s(b) $T = 1.5$ s

Figure 5 ALONGSHORE VARIATION OF $\frac{H_b}{H_b^*}$ and $\frac{\bar{\eta}_s}{\bar{\eta}_s^*}$

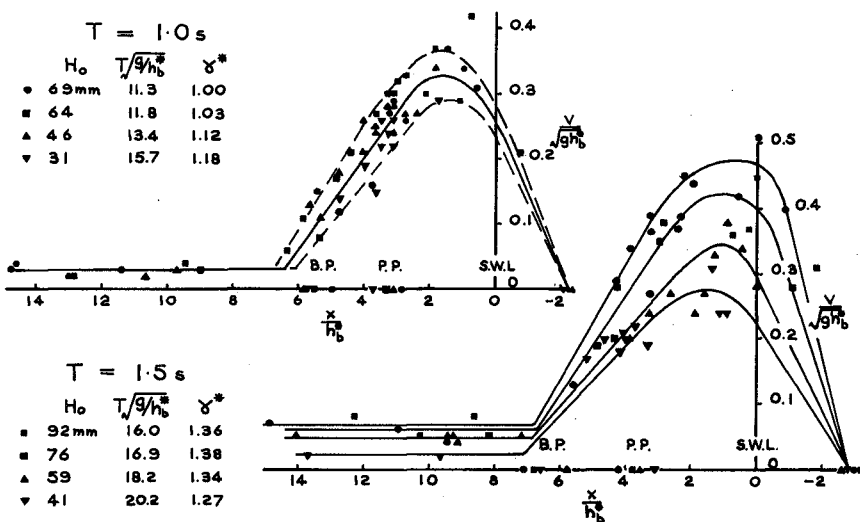


Figure 6 DIMENSIONLESS SURFACE VELOCITY PROFILES AT SECTION II

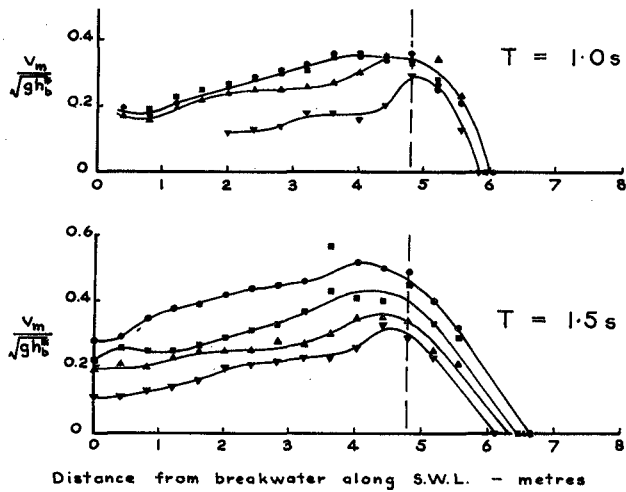
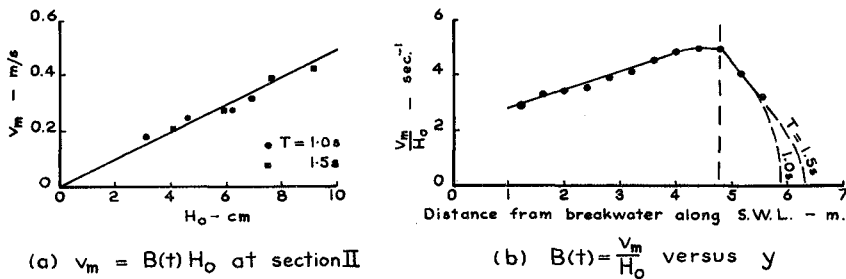
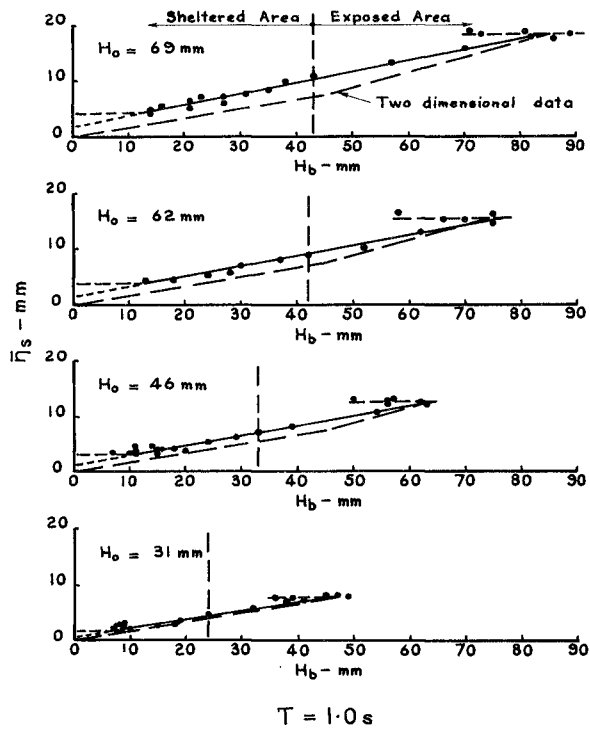


Figure 7 $\frac{v_m}{\sqrt{gh_b}}$ VERSUS ALONGSHORE DISTANCE

Figure 8 RELATIONSHIP BETWEEN v_m AND H_0 Figure 9 \bar{I}_s VERSUS H_b FOR VARIOUS H_0

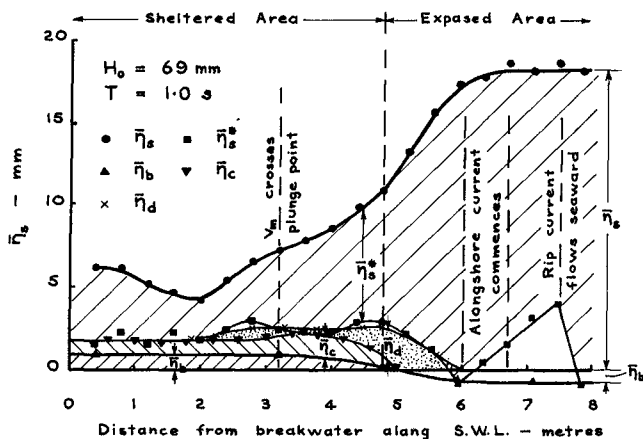


Figure 10 COMPONENTS OF WAVE SET-UP

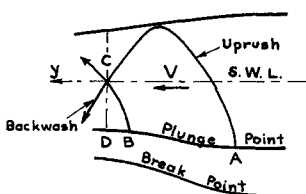
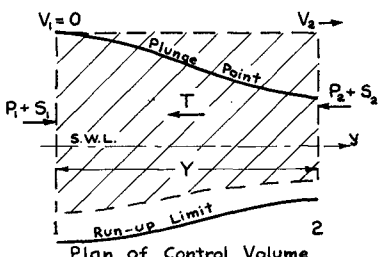


Figure 11

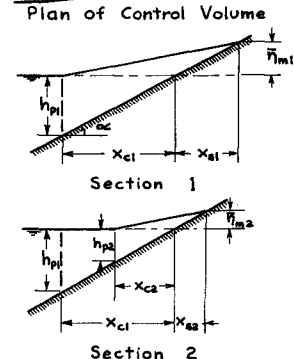


Figure 12

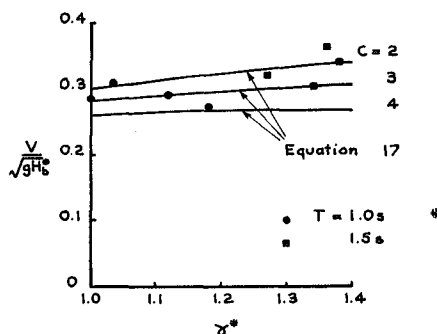


Figure 13